RESEARCH ARTICLE | MARCH 01 2011

Nanometer-scale molecular deposition using the surface Plasmon polariton interference field on a metal film

Yaling Yin; Tao Li; Ping Xu; Hua Jin; Shining Zhu

Appl. Phys. Lett. 98, 093105 (2011)
https://doi.org/10.1063/1.3560306

Nanometer-scale molecular deposition using the surface Plasmon polariton interference field on a metal film

Yaling Yin,[a] Tao Li, Ping Xu, Hua Jin, and Shining Zhu[a]
National Laboratory of Solid State Microstructures and College of Physics, Nanjing University, Nanjing 210093, People's Republic of China

(Received 26 October 2010; accepted 9 February 2011; published online 1 March 2011)

We explore the possibility of using the surface plasmon polariton interference field to deposit neutral molecules onto a silver film perforated with two double-slits. The Monte Carlo simulated results show that the deposited molecular pattern is the periodic line array with a width resolution of ~10 nm and a period of 530 nm when the molecular beam is well-collimated. Dependences of the deposition resolution on the system parameters, the potential applications and improvements are also discussed in some detail. © *2011 American Institute of Physics*. [doi:10.1063/1.3560306]

Methods for fabrication of nanometer-scale structures on solid materials have been under intensive investigations recently for their potentially nanotechnology applications. So far, methods such as optical contact lithography,[1] electron-beam lithography, imprint lithography,[2] scanning probe lithography,[3] dip-pen lithography,[4] and surface plasmonic lithography[5] have been developed in order to achieve nanometer-scale features. As the de Broglie matter wavelength of atoms or molecules is measured in picometers, their lithography resolution can approach extremely short length scales, bypassing the inherent limitations of conventional lithography. Atomic nanodeposition has been performed with various atomic species, such as Na,[6] Cr,[7] Al,[8] Yb,[9] and Fe.[10] However, it is limited to a small selection of atoms amenable to laser cooling. Also, its laser systems are complex for two-dimensional (2D) spatially periodic or quasiperiodic patterns. In this letter, we propose a special molecular nanodeposition scheme that produces the nanostructures with a resolution of ~10 nm based on the surface plasmonic optics. This scheme allows spatially complex nanostructures to be created simply and allows more molecular and atomic species to be used to form the nanostructures.

A schematic diagram of the proposed molecular nanodeposition structure is shown in Fig. 1. Two one-dimensional silver double-slits are employed to couple an incident light in free space into surface plasmon polariton (SPP) waves that propagate along the silver surface, and a SPP interference field (SPPIF) is generated across the silver surface when two counter propagating SPP waves meet together.[11,12] The neutral molecules moving in the light field will experience an induced optical dipole force that is proportional to the spatial gradient of the light intensity. Then, the molecular trajectories are modified such that a desired molecular pattern is directly deposited on the silver film. In this scheme, the deposited molecules are controlled by light just as light is controlled by optical elements in geometric optics. This method uses neither a mask nor a resist but relies on the direct deposition of molecules to form permanent nanostructures.

SPPs are surface electromagnetic waves formed by a coupling of electromagnetic field and collective oscillation of electrons at a metal or dielectric interface. The SPP dispersion relation at an interface between a semi-infinite metal and dielectric materials is $k_{SP}=(2\pi/\lambda_0)\sqrt{\varepsilon_d\varepsilon_m/(\varepsilon_d+\varepsilon_m)}$,[13] where k_{SP} is the SPP wave vector, λ_0 is the excitation light wavelength in vacuum, and ε_d and ε_m are the permittivities of a surrounding dielectric material and a metal film, respectively. According to this formula, k_{SP} is always larger than the wave vector of the excitation light in the surrounding media at the same frequency (i.e., smaller SPP wavelength). So it should make momentum compensation between the free light and the SPP wave. Grating is widely used as a convenient coupler as it can provide the appropriate reciprocal vectors to meet the momentum matching condition. As shown in Fig. 1, we employ two double-slits and each contains four slits (as a grating) actually since the periodic boundary condition is adopted. A SPP interference pattern at the silver and air interface can be formed when the distance between two double-slits are carefully adjusted to meet the standing wave condition. Using a commercial software package CST MICROWAVE STUDIO, we numerically calculate the intensity distribution at the cross section of the silver film and the results are shown in Fig. 2 under a normally incident excitation light of $\lambda_0=1095$ nm from the bottom. For calculations, the refractive index of the quartz substrate is 1.5, and that of silver is 0.19+7.89i, which is derived from the Drude mode $[\varepsilon=1-\omega_p^2/(\omega^2+i\omega\gamma)]$ with a plasma frequency $\omega_p=1.37\times10^{16}$ rad/s and collision frequency $\gamma=8.5\times10^{13}$ rad/s at $\lambda_0=1095$ nm.[14] The silver film thickness is 200 nm, the width of the silver slits is 260 nm and the distance between two slits is 800 nm. The generated SPP waves with a wavelength $\lambda=1060$ nm propagate away from the

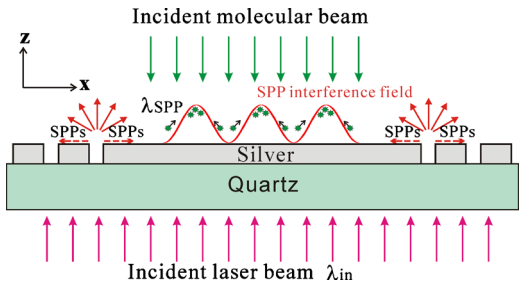

FIG. 1. (Color online) Schematic diagram of the molecular nanodeposition with the SPPIF.

[a]Authors to whom correspondence should be addressed. Electronic addresses: yalingyinwu@gmail.com and zhusn@nju.edu.cn.

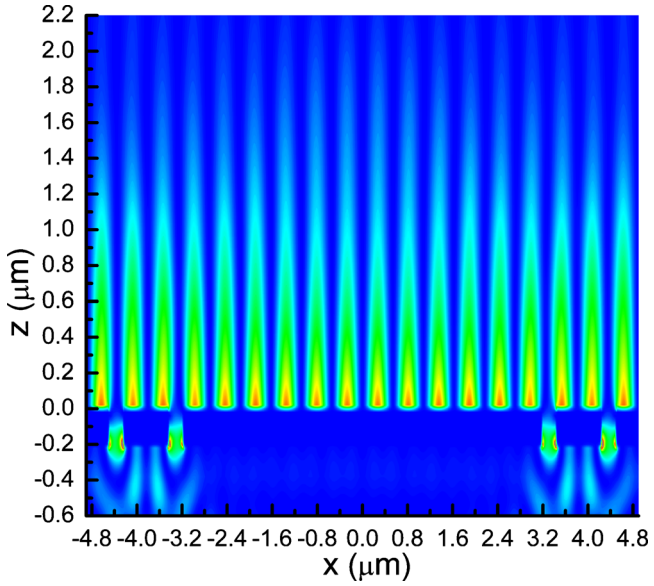

FIG. 2. (Color online) The calculated 2D light intensity distribution of the SPPIF.

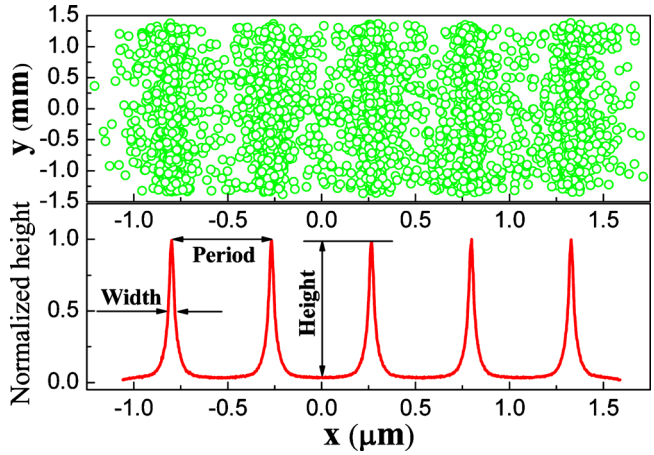

FIG. 3. (Color online) The upper plot shows the simulated spatial distribution of the deposited molecules, the lower plot gives the corresponding normalized flux distribution of the deposited molecules in the x direction.

slits and form a uniform SPPIF with a length of 6360 nm in the middle. Figure 2 shows that the periodicity of the SPPIF is half of the SPP wave (i.e., 530 nm), the decay length of the SPPIF in the z direction (defined as a length at $1/e^2$ of the light intensity at the silver surface in the z direction) is d=1720 nm, and the peak intensity is enhanced by about 5.6 times with respect to the incidence light. We also find that the intensity distribution of the SPPIF in Fig. 2 can be described with a triangle function, i.e., $I(x,z)=A[e^{-z/d}\sin(2\pi x/\lambda)]^2$, where A is the peak intensity of the SPPIF.

Molecules or atoms can be manipulated by the nonresonant optical dipole force, based on the ac stark effect. The potential energy of a molecule moving in our red-detuned SPPIF is given by $U(x,z)=-\alpha I(x,z)/(2c\varepsilon_0)$,[15] where α is the molecular average polarizability, ε_0 is the dielectric constant in vacuum, and c is the speed of light in vacuum. Molecules experience an optical dipole force $\vec{F}(x,z)=-\nabla U(x,z)$, which points to the direction of the antinodes. Each period of the SPPIF acts as a nanometer-scale molecular cylindrical lens. So molecules will accumulate on the antinodes and the molecular nanodeposition is implemented.

To test this scheme, we use the Monte Carlo method to study the dynamic process of the molecular nanodeposition. It is assumed that each molecular trajectory can be treated individually, and a large number of single molecular trajectories resulting from a statistical distribution of initial conditions can be combined to determine an output deposited molecular distribution. A cold formaldehyde (CH_2O) molecular beam with a longitudinal velocity of 65 m/s ± 20 m/s and a transverse divergence angle of θ=10 mrad is employed as the incident molecular beam because CH_2O molecules were extensively studied in cold molecular experiments, and have an adequate sticking probability on the solid surface.[16] The molecular velocities are assumed to have a Gaussian distribution in both the transverse and longitudinal directions. In our simulation, the incident laser intensity is taken to be $I_0=2.8\times10^9$ W/cm^2 that can be achieved by using a commercial optical parametric oscillation (OPO) laser.[17] The corresponding optical potential for CH_2O molecules has the maximum well depth of 0.62 K. The upper plot in Fig. 3 describes the deposited molecules in five periods of the SPPIF using the green hollow circles. It shows that most of the molecules are deposited at the antinodes of the SPPIF. Also, there are still some molecules near the antinodes as the incident molecular beam has a transverse velocity distribution. The lower plot in Fig. 3 is the corresponding normalized statistical distribution of the deposited molecules. We can see that the deposited molecular lines are nearly parallel and have a period of 530 nm, the corresponding average full width at half maximum line width W is as small as 35.5 nm. The simulated results also show that the whole deposition process lasts about 4.5 ± 2.1 ns.

In this scheme, the SPPIF works as a molecular cylindrical lens to focus the molecular beam onto the silver film. The light intensity of the SPPIF and its optical potential for CH_2O are the positional dependence in the transverse direction and the corresponding optical dipole force (i.e., a restoring force) is proportional to the transverse position of the deposited molecules. So, we can deduce that the final position of the deposited molecules on the silver film is related to the initial molecular position and its transverse velocity as well as the light intensity of the SPPIF. As soon as the molecular focused line is just on the silver film, the deposited molecular line width W will be the narrowest. We study the dependence of the line width W on the incident light intensity I_0 and the divergence angle θ of the molecular beam, and the simulated results are shown in Fig. 4. In Fig. 4(a), the divergence angle of incident molecular beam and its longitudinal velocity are θ=10 mrad and 65 m/s ± 20 m/s, respectively. Figure 4(a) confirms that the deposited line width W falls to 35.5 nm that is the narrowest when the incident light intensity equals to $I_0=2.8\times10^9$ W/cm^2, which is defined as the optimal light intensity I_{op}. The line width W becomes broader when I_0 is lower/larger than I_{op}, as the molecular focused line is below/upper the silver film. So the proper incident light intensity should be considered when the parameters of the incident molecular beam and the structure of the silver film are fixed in the experiment. The simulated line width W in the case of different divergence angles are shown in Fig. 4(b), where I_0 equals to I_{op}. It is clear that the line width W monotonically increases with the increasing of

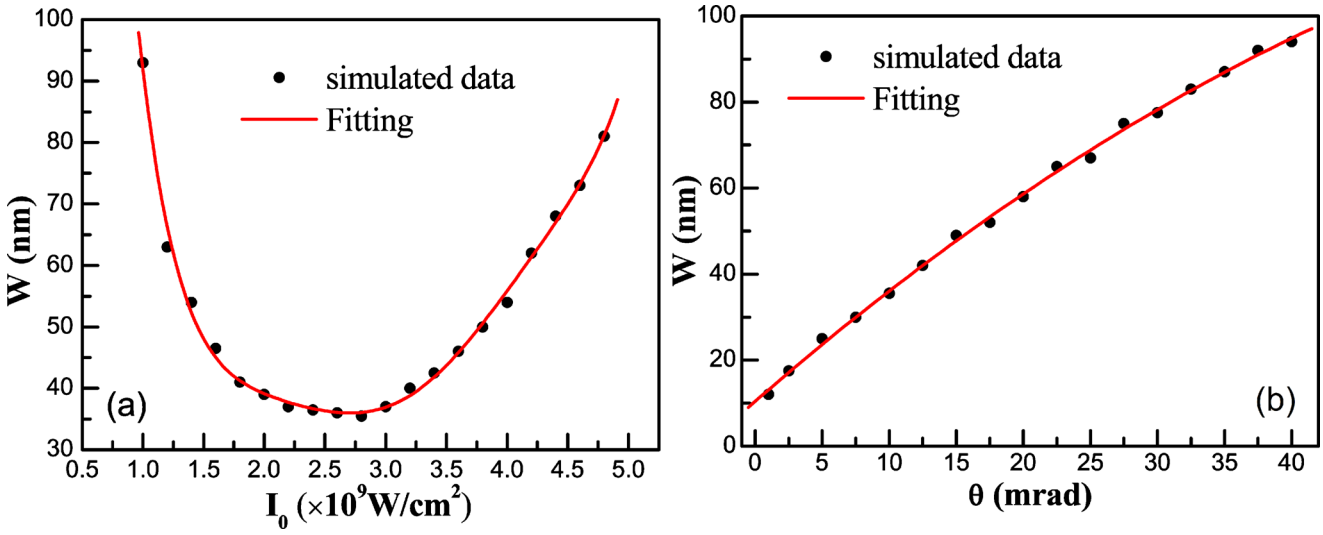

FIG. 4. (Color online) The dependence of line width W on (a) the light intensity I_0 of the incident laser beam and (b) the divergence angle θ of the incident molecular beam.

the divergence angle θ. The line width falls to $W=12$ nm when $\theta=1$ mrad. This is because the transverse kinetic energy of the deposited molecules depends on the divergence angle of the molecular beam. The transverse velocity changes the oscillatory periods of molecules in the transverse direction, and some molecules are deposited near the antinodes. So the deposited molecular patterns can be made finer and narrower by using a well-collimated molecular beam, which can be obtained by the magnetic/electric hexapole field or geometrical skimmer method in the experiment.

For the purpose of molecular nanodeposition with a lower light intensity, a grazing angle of the incident molecular beam may offer a number of significant advantages.[18] Also, we can invite a much colder molecular beam to implement the nanodeposition. In former lithography, a complex pattern must be fabricated with complex laser light path. Multiple laser beams have to be very precisely aligned and phase-controlled. Our scheme, on the other hand, does not suffer from this limitation because it can be implemented by designing the proper 2D distribution of the silver slits with only one excitation laser beam, and dynamically adjusting the wavelength, polarization and incident angle of the excitation light beam.[11,12] So molecular nanodeposition with a periodic or quasi-periodic, even more complicated 2D pattern can be realized.

In conclusion, we have described a molecular nanodeposition scheme that uses the SPPIF to focus molecules onto the silver film directly on the sub-100 nm scale. Monte Carlo simulation shows that a molecular nanodeposition with a line width of ~10 nm can be realized when the incident CH_2O molecular beam is well-collimated and the incident light intensity is taken to be an optimal value. This scheme is general, and could be used to deposit polarizable atoms or molecules, metals, semiconductors, and biomolecules[19] onto the substrate with complex 2D or three-dimensional patterns. This scheme could also be used to form some microstructures with special electric, magnetic, and optical properties. The distribution of the deposited molecules is determined by the SPP field distribution, so the produced molecular pattern can be used as a measure of the near-field light intensity distribution that cannot be detected directly by conventional optical instruments. Also, the produced molecular pattern can be used as a length calibration of standards for the nanometer-scale structure in the field of nanometrology.[20]

The authors are grateful to Dr. Qi Zhou for the helpful discussions. The authors acknowledge support from the National Natural Science Foundation of China under Grant Nos. 10904060, 10974090, and 11021403, the Jiangsu Planned Projects for Postdoctoral Research Funds.

[1]M. M. Alkaisi, R. J. Blaikie, and S. J. Mcnab, Microelectron. Eng. **53**, 237 (2000).
[2]R. S. Dhaliwal, W. A. Enichen, S. D. Golldaday, M. S. Gordon, R. A. Kendall, J. E. Lieberman, H. C. Pfeiffer, D. J. Pinckney, C. F. Robinson, J. D. Rockrohr, W. Stickel, and E. V. Tressler, IBM J. Res. Dev. **45**, 615 (2001).
[3]E. B. Cooper, S. R. Manalis, H. Fang, H. Dai, K. Matsumoto, S. C. Minne, T. Hunt, and C. F. Quate, Appl. Phys. Lett. **75**, 3566 (1999).
[4]R. D. Piner, J. Zhu, F. Xu, S. Hong, and C. A. Mirkin, Science **283**, 661 (1999).
[5]W. Srituravanich, N. Fang, C. Sun, Q. Luo, and X. Zhang, Nano Lett. **4**, 1085 (2004).
[6]G. Timp, R. E. Behringer, D. M. Tennant, and J. E. Cunnungham, Phys. Rev. Lett. **69**, 1636 (1992).
[7]J. J. McClelland, R. E. Scholten, E. C. Palm, and R. J. Celotta, Science **262**, 877 (1993).
[8]R. W. McGowan, D. M. Giltner, and S. A. Lee, Opt. Lett. **20**, 2535 (1995).
[9]R. Ohmukai, S. Urabe, and M. Watanabe, Appl. Phys. B: Lasers Opt. **77**, 415 (2003).
[10]E. te Sligte, B. Smeets, K. M. R. van der Stam, R. W. Herfst, P. van der Straten, H. C. W. Beijerinck, and K. A. H. van Leeuwen, Appl. Phys. Lett. **85**, 4493 (2004).
[11]Z. W. Liu, Q. Wei, and X. Zhang, Nano Lett. **5**, 957 (2005).
[12]Z. W. Liu, Y. Wang, J. Yao, H. Lee, W. Srituravanich, and X. Zhang, Nano Lett. **9**, 462 (2009).
[13]H. Raether, *Surface Plasmons on Smooth and Rough Surfaces and on Gratings* (Springer, Berlin, 1988).
[14]T. Li, H. Liu, S. M. Wang, X. G. Yin, F. M. Wang, S. N. Zhu, and X. Zhang, Appl. Phys. Lett. **93**, 021110 (2008).
[15]Y. L. Yin, Q. Zhou, L. Z. Deng, Y. Xia, and J. P. Yin, Opt. Express **17**, 10706 (2009).
[16]L. D. van Buuren, C. Sommer, M. Motsch, S. Pohle, M. Schenk, J. Bayerl, P. W. H. Pinkse, and G. Rempe, Phys. Rev. Lett. **102**, 033001 (2009).
[17]Sunlite™ EX OPO, Continuum Inc., see http://www.continuumlasers.com/products/tunable_Sunlite_EX.asp.
[18]R. J. Gordon, L. Zhu, W. A. Schroeder, and T. Seideman, J. Appl. Phys. **94**, 669 (2003).
[19]R. Quidant and C. Girard, Laser Photonics Rev. **2**, 47 (2008).
[20]S. Gonda, T. Doi, and T. Kurosawa, Rev. Sci. Instrum. **70**, 3362 (1999).